

A Unified Optic Nerve Head and Optic Cup Segmentation Using Unsupervised Neural Networks for Glaucoma Screening

Zeinab Ghassabi, Jamshid Shanbehzadeh, Kouroos Nouri-Mahdavi

Abstract— Segmentation of retinal anatomical features such as optic nerve head (ONH) and optic cup, the brightest area in the center of ONH which is devoid of neural elements, is a prerequisite for computer-aided diagnosis and follow-up of glaucoma. The ONH segmentation methods, which imposed shape and intensity constraints, are unable to identify ONH and optic cup boundaries at the same time. On the other hand, recent efficient supervised learning-based methods, which provide a unified system, require combination of many informative features as their inputs, as well as ground truth for the training phase. This paper uses a saliency map including color, intensity and orientation contrasts as the input of a winner-take-all neural network, and color visual features as the input of a self-organizing map neural network to segment ONH and optic cup, simultaneously. Our method is evaluated on a database of 205 ocular fundus images provided by local eye hospitals and publicly available image databases RIMONE and DIARETDB0 comprising 60 non-glaucomatous and 145 glaucomatous images. The ground truth is provided by two expert ophthalmologists. The method attained an average overlapping error of 9.6% and 25.1% for ONH and cup segmentation, respectively. Cup-to-disc area ratio (CDR) is computed for glaucoma assessment. The mean and standard deviation of the CDR differences between our method and the ground truth in all images are 0.11 and 0.09, respectively.

I. INTRODUCTION

Glaucoma is the second worldwide cause of blindness. Early detection of glaucoma can prevent irreversible visual loss. Enlargement of the optic cup area compared to the optic nerve head (ONH) area is a primary indicator of glaucoma [1]. Hence, a high cup-to-disc (CDR) ratio [1,2], which expresses the proportion of the ONH that is devoid of retinal ganglion cell axons, could indicate presence of glaucoma. Precise segmentation of the ONH to derive a set of pixels that belongs to either ONH or optic cup and estimation of CDR can therefore, contribute to early detection of glaucoma. Segmentation of the ONH and optic cup is a challenging task due to many vessels crossing the ONH, intensity variation within the ONH and its vicinity, and varied configurations of the optic cup. For example, presence of tissue atrophy around the ONH boundary (peripapillary atrophy) distort correct delineation of the ONH shape and emerging vessels in ONH region may obscure portions of optic cup [2,3].

Much of existing work has mainly focused on ONH segmentation with only few attempts at cup segmentation [4].

Zeinab Ghassabi, PhD, is with the Stein Eye Institute, UCLA, LA, CA, USA (corresponding author's e-mail: zghassabi@jsei.ucla.edu).

Jamshid shanbehzadeh, PhD, is with the Engineering Department, Kharazmy University, Tehran, Iran (Jamshid@khu.ac.ir).

Kouroos Nouri-Mahdavi, MD, is with Stein Eye Institute, UCLA, LA, CA, USA. (e-mail: nouri-mahdavi@jsei.ucla.edu).

ONH segmentation methods can be grouped into template matching algorithms, appearance-based methods, deformable models and machine-learning methods [4]. Template matching methods [5,6] computed the cross-correlation of a circular template like circular Hough transform [3,5] with fundus images to detect the ONH boundary. Since templates are based on the circular shape of ONH, localizing ONH is impossible in the presence of peripapillary atrophy, which can distort the shape of ONH. Appearance-based methods search regions within fundus images with the highest number of the brightest pixels [7] or the highest intensity variation [8] due to confluence of vessels in ONH. These methods are sensitive to uneven illumination, presence of large bright lesions and strongly visible choroidal vessels [4,5]. Concerning deformable models, performance of ONH contour detection based on GVF-snake [9] and Chan-Vese active contour model [10] depends on the differentiation of ONH edges from peripapillary atrophy surrounding ONH [11]. Recently, learning-based methods consisting of artificial neural networks, fuzzy c-means clustering (FCM) method [12], k-nearest neighbor [13] and deep learning [14] have been used for ONH and cup detection, simultaneously. Although these methods do not impose any shape constraints on the segmentation results, they require either a complex feature extraction process to provide relevant and distinctive input features or fine tuning of several hyperparameters, as well as ground truth for training phase [12,13,14]. We propose a unified ONH and cup segmentation consisting of two consecutive unsupervised neural networks.

II. PROPOSED OPTIC NERVE HEAD AND OPTIC CUP SEGMENTATION FRAMEWORK

Fig. 1 shows a graphical overview of our method. We first identified region of interest (ROI) including ONH by winner-take-all (WTA) neural network [15]. Then, vessel inpainting converts ROI to a representation suited for ONH and cup segmentation. A color reduction process on ROI by combining HSV color-space and self-organizing map (SOM) neural network [16] determines corresponding reduced color or class of each pixel as the optic cup, ONH or background pixel.

A. Region of Interest Detection

The most salient area of a fundus image I , which shows highly intensity, color and orientation contrasts to the surrounding parts, likely contains the ONH. Global thresholding methods are ineffective to localize the ONH as the brightest region of fundus in the presence of white lesions similar to the ONH, and weak contrast and blurred images [17]. Therefore, we employed an effective method [15] which combined a saliency map and winner-take-all (WTA) neural network to select the most likely location of the ONH in

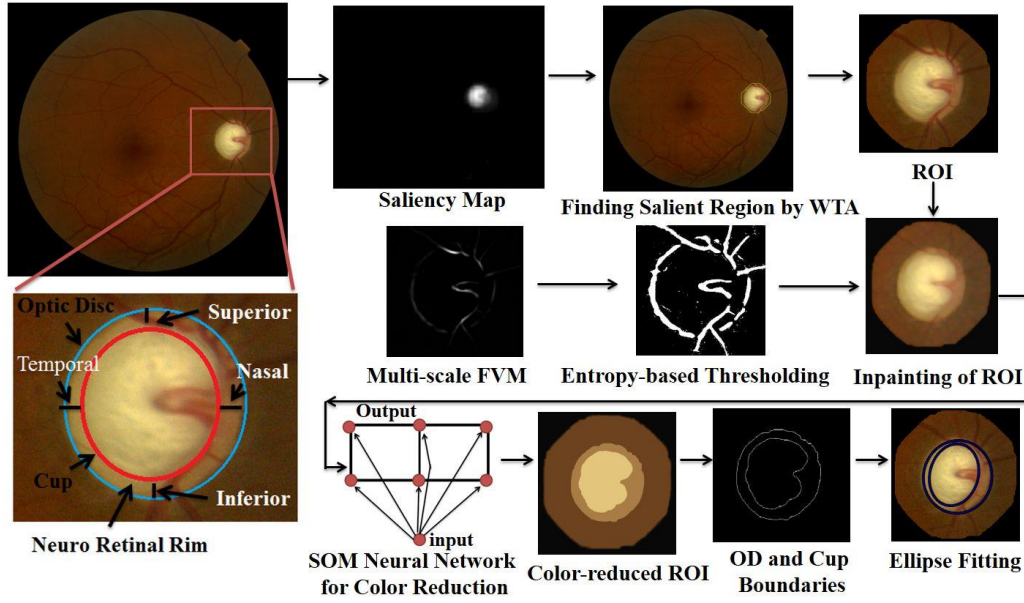


Figure 1. Algorithm review for a glaucomatous fundus image. Color-reduced ROI includes fundus background, rim and optic cup

fundus from the saliencies of pixels. This poses the problem of finding ROI as a classification problem of a saliency map. A saliency map based on color, intensity and orientation features is constructed, so that the highest salient region is likely to contain the ONH, and other pixels with lower saliency are relegated to the background. A saliency value for a pixel x can be calculated by linearly combining the contrast maps

$$SP(x) = \sum_{l=1}^L \sum_{y \in W} (\gamma_{CI} S_{CI}^l(x, y) + \gamma_O S_O^l(x, y)) \quad (1)$$

at L (equal to 3) scales in the Gaussian image pyramid. γ is the pixel belonging to a 3×3 window W centered at x . S_{CI}^l and S_O^l denote color-intensity and orientation contrasts between x and y , respectively. γ_{CI} and γ_O are weighting coefficients equal to 1. Color contrast was computed via red, green, blue and yellow channels. The gray-level image was used to compute intensity contrast according to [28]. Orientation contrast, which evaluates the degree of homogeneity or heterogeneity, was calculated by Gabor filters [15].

Once, saliency map was constructed, WTA scans the saliency map for the most salient location and returns its coordinate (Figure 1). To provide sufficient context about the surrounding retinal background, we set the width of ROI to about twice the width of the average ONH.

B. Vessel Inpainting of ROI

The performance of simultaneous ONH and optic cup segmentation depends on the differentiation of ONH and cup edges from other structures. The smooth and narrow temporal region of the retinal rim provides little information for further color reduction step. Furthermore, the confluence of outgoing vessels in ROI reduces the accuracy of ONH and optic cup detection, so that they obscure the nasal side of retinal rim.

To address this, the ROI inpainting method removes the influence of vessels by replacing vessel pixels with their adjacent ONH or cup pixels. Meanwhile, it refines edge characteristics like ONH and cup boundaries. On one hand, the proposed inpainting method discriminates ONH from peripapillary atrophy or background pixels. On the other hand, it discerns a narrow retinal rim with non-obvious temporal region to highlight the cup. First, we obtained a binary mask including vessels, ONH and cup boundaries by a multi-scale filter process, Frangi Vesselness Measure (FVM) [18], followed by entropy-based thresholding [17]. Further, the ROI pixels are altered using the following steps:

- The mask, I_{mask} , is applied on ROI in the RGB color space according to $I_1 = (1 - I_{mask}) * ROI$.
- A color morphological closing $I_2 = (I_1 \oplus b) \ominus b$ followed by opening $I_2 = (I_2 \ominus b) \oplus b$ with a disk shape structuring element b (with size of 12 and 3 respectively) are applied to fill the intensities of the mask pixels in three RGB channels and to distinguish ONH and cup boundaries.
- The color image is smoothed by a median filter with a 5×5 neighborhood dimension in three RGB channel $(I_{inpt} = med(I_2, [5, 5]))$ to provide homogeneous regions inside the rim and cup.

C. SOM-based Color Reduction

Instead of exaggerating elaborate features for pixel-based classification [13,14], we pose the problem of ONH and optic cup segmentation as a color reduction problem in the ROI by SOM neural network [16]. First, the RGB color space of ROI is represented in HSV (Hue, Saturation, brightness Value) color space [16] since HSV is more sensitive to high contrast areas and to luminance. Next, a weighted form of three colors [3 2 1] for each color point

$X = [H, S, V] \in R^3$ is presented to input of SOM. The SOM network is comprised of a layer of m neurons ordered in a 2-D grid feature map (Fig. 1). By default, we set the size of SOM map to 2×3 with a hexagonal topology. SOM employs competitive learning, so that in an iterative way, X is presented to the network, and the neuron with minimum Euclidian distance between its weight vector $w_i = [H_i^{new}, S_i^{new}, V_i^{new}] \in R^3$ and input vector is declared as the winner according to

$$j = \arg \min_i \|X - w_i(t)\| \quad (2)$$

The weights of the winning neuron j and its neighboring neurons i will be modified as

$$w_i(t+1) = w_i(t) + \eta(t)h_{ij}(X, t)[X(t) - w_i(t)] \quad (3)$$

where t is the learning step, $\eta(t) = \eta_0 e^{-\frac{t}{\tau}}$ is a monotonically decreasing learning factor with $\eta_0 = 0.08$, and

$$h_{ij}(x, t) = e^{\frac{-d_{ij}^2}{2\sigma(t)^2}}, \text{ with } \sigma(t) = \sigma_0 e^{-\frac{t}{\tau}}, \tau = \frac{1000}{\log \sigma_0}, \text{ is a Mexican}$$

hat kernel, so that its values drops in a Gaussian manner as the distance between the map neuron i and its neighbor neuron j , d_{ij} , increases. σ_0 is the radius of the grid. The maximum number of iterations for SOM learning is 200.

Since the input pixels X are assigned to several clusters, the points in each cluster are averaged to obtain the cluster centroid or representative color that all input points in that cluster are mapped to. Finally, a resulting cluster that contains the corresponding center of the salient region or the brightest color was regarded as optic cup cluster. Consequently, the closest cluster to the cup is the second brightest region or ONH. Then, CDR is estimated after computing the best fitted ellipse using elliptical Hough transform for both the cup and ONH [4].

III. EXPERIMENTAL RESULTS

We used four datasets to evaluate the proposed optic cup and ONH segmentation method, and glaucoma assessment system. The first dataset consists of 115 glaucomatous and 52 non-glaucomatous fundus images with a resolution of 2048 by 1536 pixels from Labbafi Nedjad hospital of Iran [19,20]. We also selected 18 fundus images randomly from two publicly available databases RIMONE [21] and DIARETDB0 [22]. Additionally, 20 fundus images with primary open angle glaucoma [1] were taken from the research database at Stein Eye Institute in UCLA. Fig. 2 shows the proposed ONH and cup segmentation results of two fundus images. ROI detection method localized ONH correctly in all images. Two clinicians provided manual boundary as “ground truth” for ONH and optic cup. The overall performance of ONH and cup segmentation is evaluated by measuring the overlapping error [4] as

$$E = 1 - \frac{\text{Area}(S \cap G)}{\text{Area}(S \cup G)} \quad (4)$$

where S and G are the segmented ONH/optic cup and ground truth, respectively. Table I and Table II demonstrate

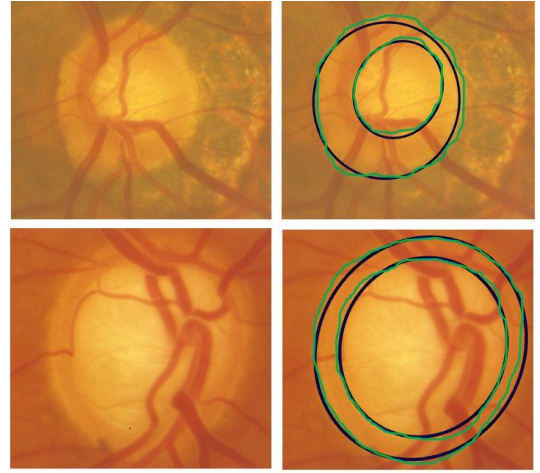


Figure 2. Optic cup and OD detection manually or ground truth (green), and proposed method after ellipse fitting

the percentage of fundus images per E interval and mean overlapping error μ_E by these methods. Table I shows that the proposed method achieves higher percentage of images with small errors ($E \leq 0.2$) than circular Hough transform [6], GVF-snake [9], FCM clustering and multilayer neural network [12] for ONH segmentation. Table II illustrates promising results from the proposed method in comparison to r-bend [10] and spatially weighted fuzzy-c means (SWFCM) clustering [11] for cup segmentation. The proposed method has reduced μ_E in comparison to all other ONH and cup segmentation methods. According to [12], for each pixel of ROI, combination of various features such as pixel values (RGB components), local intensity and orientation contrast, median value in surrounding pixels, Sobel edge information and red-channel of vessel erased image were employed as inputs of FCM and neural network. Despite using several input features by FCM and neural network, the proposed method classified ONH pixels correctly with only weighted form of HSV color features. This is due to effective inpainting which provide suitable color features. Moreover, the neighborhood function $h_{ij}(x, t)$ of SOM learning rule shrinks with time, the weight updating takes place on a global scale at the beginning of learning and then, they converge to local estimates due to few neighboring neurons. This leads to maximum similarity between input image to SOM output, which is a reduced color image, so that non-dominant colors are eliminated or weakened and minimum distortion of structural information, namely ONH and cup boundaries, occurs. We attained the best similarity between input ROI image and reduced color image with a 2×3 feature map in the SOM neural network, for ONH and cup segmentation.

We used the absolute CDR error [4]

$$\delta = |CDR_{GT} - CDR_E| \quad (5)$$

where δ is the difference between the estimated CDR_E and ground truth CDR_{GT} , to evaluate the accuracy of CDR for glaucoma screening. Table III shows the mean error μ and the standard deviation σ of the error in estimating CDR for glaucomatous, non-glaucomatous and all images. Small

mean error and standard deviation of the CDR error indicate high accuracy of our method in glaucoma assessment.

IV. CONCLUSION

This paper proposed a unified ONH and cup segmentation method for glaucoma assessment. The core of the method is color reduction by self-organizing map neural network to determine the corresponding reduced color or class of the input pixels. Thanks to the saliency map detection, our method can deal with optic disc localization on fundus images that contain bright lesions. Additionally, inpainting eliminates obstruction from outgoing vessels and lead to improved contours of the ONH and cup for further robust color reduction. Hence, the entire method is efficient even in the presence of non-obvious neuroretinal rim, peripapillary atrophy and low intensities of the optic cup. The experimental results confirm the superior performance of the proposed ONH and cup detection method in comparison to other methods in terms of overlapping error. In future, we will directly provide a real-time unified segmentation system without coarse localization of ONH at first.

TABLE I. PERCENTAGE OF IMAGES FOR E INTERVAL AND μ_E FOR VARIOUS ONH SEGMENTATION METHODS

Methods	$E \leq$					μ_E
	0.05	0.1	0.15	0.2	0.25	
<i>Hough transform</i>	11%	48%	70%	78%	57%	12.8%
<i>GVF-snake</i>	15%	60%	79%	91%	92%	10.4%
<i>FCM</i>	14%	60%	78%	90%	92%	10.7%
<i>Neural Network</i>	14%	61%	80%	90%	93%	10.1%
<i>Proposed method</i>	18%	67%	85%	93%	96%	9.6%

TABLE II. PERCENTAGE OF IMAGES FOR E INTERVAL AND μ_E FOR VARIOUS OPTIC CUP SEGMENTATION METHODS

Methods	$E \leq$					μ_E
	0.01	0.2	0.3	0.4	0.5	
<i>r-bend</i>	0%	2%	23%	53%	72%	40.1%
<i>SWFCM</i>	5%	26%	53%	81%	92%	33.4%
<i>Proposed Method</i>	9%	39%	64%	90%	95%	25.1%

TABLE III. MEANS AND STANDARD DEVIATION OF CDR AREA ERROR BETWEEN THE PROPOSED METHOD AND THE GROUND TRUTH

Images	μ	σ
<i>Non-glaucoma</i>	0.21	0.12
<i>Glaucoma</i>	0.08	0.07
<i>Total</i>	0.11	0.09

ACKNOWLEDGMENT

The authors would like to thank Mrs. Zohreh Salimi in the Shahid Labbafi Nedjad Hospital of Iran for providing the dataset.

REFERENCES

- [1] P. N. Schacknow, and J. R. Samples., The Glaucoma Book, A Partial, Evidence-Based Approach to Patient Care, Springer, 2010.
- [2] A. Poshtyar, Z. Ghassabi, J. Shanbehzadeh, "Detection of Optic Disc Center and Macula using Spatial Information of Optic cup", 4th International Conf. on Biomedical Engineering and Informatics (BMEI), pp. 255-258, 2011.
- [3] A. Aquino, M. E. Gegúndez-Arias, and D. Marín, "Detecting the Optic Disc Boundary in Digital Fundus Images Using Morphological, Edge Detection, and Feature Extraction Techniques", IEEE Trans. On Med. Imag., vol. 29, no. 11, pp. 1860-1869, Nov. 2010.
- [4] J. Cheng, J. Liu, Y. Xu, and et al., "Supapixel Classification Based Optic Disc and Optic Cup Segmentation for Glaucoma Screening", IEEE Trans. On Med. Imag., vol. 32, no. 6, June 2013.
- [5] T. Kauppi, H. Kälviäinen, "Simple and Robust Optic Disc Localisation Using Colour Decorrelated Templates", Advanced Concepts for Intel. Vision Sys., vol. 5259, Lecture Notes in Comput. Sci., pp 719-729, 2008.
- [6] S. Sekhar, W. Al-Nuaimy, and A. K. Nandi, "Automated localisation of retinal optic disk using hough transform", 5th IEEE Int. Symp. Biomed. Imag., pp. 1577-1580, 2008
- [7] H. Narasimha-Iyer, A. Can, C. V. Stewart, B. Roysam, H.L. Tanenbaum, A. Majerovics and H. Singh, "Robust detection and classification of longitudinal changes in color retinal fundus images for monitoring diabetic retinopathy", IEEE Trans. Biomed. Eng., vol. 3, no. 6, 2006.
- [8] C. Sinthanayothin, V. Kongbunkiat, S. Phoojaruenchanachai and A. Singalavanija, "Automated screening system for diabetic retinopathy", Proc. 3rd Int. Symp. on Img. and Signal Proc. and Analysis, pp. 915-920, 2003.
- [9] A. Osareh, M. Mirmehdi, B. Thomas, R. Markham, Colour morphology and snakes for optic disc localization, in: Proceedings of Medical Image Understanding and Analysis, MIUA, pp. 21-24, 2002.
- [10] G.D. Joshi, J. Sivaswamy, K.P.R. Karan, R. Krishnadas, Optic disk and cup segmentation from monocular color retinal images for glaucoma assessment, IEEE Trans. Med. Imaging, vol. 30, no. 6, pp. 1192-1205, 2011.
- [11] P. S. Mitapalli, G. B. Kande, "Segmentation of optic disk and optic cup from digital fundus images for the assessment of Glaucoma", Biomed. signal process. and control, vol. 24, pp 34-46, 2016.
- [12] C. Muramatsu, T. Nakagawa, A. Sawada, Y. Hatanaka, et al., "Automated segmentation of optic disc region on retinal fundus photographs: Comparison of contour modeling and pixel classification methods", Comput. Methods Prog. Biomed., vol. 101, no.1, pp. 23-32, 2011.
- [13] M.D. Abramoff, W.L.M. Alward, E.C. Greenlee, et al., "Automated segmentation of the optic disc from stereo color photographs using physiologically plausible features", Invest. Ophthalmol. Vis. Sci., vol. 48, pp. 1665-1673, 2007.
- [14] H. Fu, J. Cheng, and et al. "Joint Optic Disc and Cup Segmentation Based on Multi-label Deep Network and Polar Transformation" IEEE Transactions on Medical Imaging, 2018
- [15] Y. Sun, R. Fisher, "Object-based visual attention for computer vision", Artificial Intel., vol. 146, no. 1, pp. 77-123, 2003.
- [16] L. P. Chen, Y. G. Liu, Z. X. Huang, Y. T. Shi, "An improved SOM algorithm and its application to color feature extraction", Neural Comput & Applic, vol. 24, no. 7, pp. 1759-1770, 2013.
- [17] S. Omid, Z. Ghassabi, J. shanbehzadeh, SS. Ostadzadeh, "Optic Disc Detection in High-Resolution Retinal Fundus Images by Region Growing", IEEE int. Conf. BMEI, 2015.
- [18] A. F. Frangi, W. J. Niessen, K. L. Vincken, and M. A. Viergever, "Multi-scale Vessel Enhancement Filtering", Medical Image Computing Computer-Assisted Intervention (MICCAI), pp. 130-137, 1998.
- [19] Z. Ghassabi, J. shanbehzadeh, A. Mohammadzadeh, SS. Ostadzadeh, "Colour retinal fundus image registration by selecting stable extremum points in the scale-invariant feature transform detector", IET imag. Process., vol. 9, no. 10, pp. 889-900, 2015.
- [20] Z. Ghassabi, J. Shanbehzadeh, A. Mohammadzadeh, "A structure-based Region Detector for high resolution retinal fundus image registration", Biomedical signal processing and control, vol. 23, pp. 52-61, 2016
- [21] F. Fumero, S. Alayon, J.L. Sanchez, J. Sigiut, M. Gonzalez-Hernandez, "RIM-ONE: An Open Retinal Image Database for Optic Nerve Evaluation", IEEE Comput. Med. Sys. (CBMS), pp. 1-6, 2011.
- [22] DIARETDB0, <http://www2.it.lut.fi/project/imageret/diaretdb0/>